

COLOR HISTOGRAM DIFFUSION FOR IMAGE ENHANCEMENT

Taemin Kim

Intelligent Robotics Group, NASA Ames Research Center, Moffett Field, CA 94035
taemin.kim@nasa.gov

ABSTRACT

Various color histogram equalization (CHE) methods have been proposed to extend grayscale histogram equalization (GHE) for color images. In this paper a new method called “histogram diffusion” that extends the GHE method to arbitrary dimensions is proposed. Ranges in a histogram are specified as overlapping bars of uniform heights and variable widths which are proportional to their frequencies. This diagram is called the “vistogram.” As an alternative approach to GHE, the squared error of the vistogram from the uniform distribution is minimized. Each bar in the vistogram is approximated by a Gaussian function. Gaussian particles in the vistogram diffuse as a nonlinear autonomous system of ordinary differential equations. CHE results of color images showed that the approach is effective.

Index Terms— Color image processing, Contrast enhancement, Mixture of Gaussians

1. INTRODUCTION

A rapid transition from grayscale to color images has been undergone in the last three decades. There has been an explosion of color algorithms that ranges from direct extensions of grayscale methods to more sophisticated techniques which exploit correlations among color bands. The grayscale histogram equalization (GHE) is one of the simplest and most effective methods for contrast enhancement in many image-processing applications [1][2]. The method is useful in processing images with backgrounds and foregrounds that both are bright or dark. For example, GHE of the Lena image is shown Figure 1. The contrast of the equalized image shown in Figure 1 (b) is enhanced conspicuously. The histogram equalization technique are useful in alleviating the photometric disparity of different images from the same scene, e.g., in stereopsis.

The extending of GHE to color images, i.e., color histogram equalization (CHE), is not simple. Various methods have been proposed to address this issue. Those approaches can be categorized as: i) marginal (or



(a) Lena image (b) GHE equalized image
Figure 1: Grayscale histogram equalization of the Lena Image.

conditional) CHE, and ii) multidimensional histogram equalization (MHE). Assuming the marginal histograms of a color image are independent from other aspects of the histogram, the marginal CHE applies GHE directly to them [3][4][5][6]. The techniques provide fast and efficient algorithms to equalize histograms. However, they do not consider the correlation between different bands. Multidimensional histogram equalization methods reformulate GHE not to use the order information, thus, making it extendable to multi-dimension [1][7][8][9]. Approximating the histogram by a mixture of isotropic Gaussians (MIG), Kim and Yang proposed another CHE method to fit PDFs and generate an almost uniform histogram [10][11]. However, to sustain the continuity of mapping the method required special care to the scale parameter, which could be difficult to accomplish.

The aims of the research are two-fold: i) to establish a new concept of histogram diffusion which is dynamically and numerically stable, and ii) to apply the method to image enhancement, i.e., CHE. The histogram of any dimension is approximated by a MIG and thus provides the smooth probability density function. The disparity between the MIG and the target distribution function in terms of the squared error provides a potential energy function for the histogram diffusion, which has to be minimized. Adding kinetic energy of Gaussian particles, the histogram diffusion process is formulated as a nonlinear autonomous system of ordinary differential equations (ODEs) [16]. The proximity of Gaussian particles reduces the computational time in a linear order fashion. Examples of color histogram diffusion demonstrate its effectiveness in CHE.

2. HISTOGRAM DIFFUSION

A histogram of a grayscale image is a graphical display of tabulated frequencies, which are obtained by counting the number of pixels of a given set of intensity ranges. The frequency of intensity ranges are usually represented as non-overlapping rectangular bars of uniform widths and variable heights which are proportional to the magnitude of represented quantities. For example, a 1D histogram in the normalized domain $D=[b^-, b^+]$, where $b^\pm := \pm 0.5$, is shown in Figure 2 (a). On the other hand overlapping bars of uniform heights but variable widths represent a histogram where the heights of overlapped bars are proportional to the degree of overlap (Figure 2c). The new diagram is called a “vistogram.” This is to indicate that the volume of bars in multi-dimension changes according to their frequencies.

To understand the GHE method and the concept of vistogram the centralized GHE method is introduced. For a given histogram represented by probability $\{p_i\}_{i=1}^n$ at points $\{x_i\}_{i=1}^n$ in the domain D , the centralized GHE method is

$$x_i^* = \frac{1}{2} \sum_{k=1}^n p_k \operatorname{sgn}(x_i - x_k). \quad (0)$$

Application of the centralized GHE method to the histogram in Figure 2 (a) is presented in Figure 2 (b). Correspondingly, the equalized vistogram shows the perfect uniform distribution (Figure 2d):

$$x_{i+1}^* - x_i^* = \frac{p_{i+1} + p_i}{2} \text{ for } i=1, 2, \dots, n. \quad (0)$$

The histogram equalization, therefore, can be achieved by removal and minimization of overlapping and vacant areas of the corresponding vistogram.

Minimizing the squared error of vistogram provides an alternative to GHE and can be extended to CHE. In fact, (0) is a minimizer of the squared errors. However, it does not guarantee the continuity of transformation. This is the result of heavy overlap of bars in the vistogram because the squared error has plateaus in some places. To avoid these

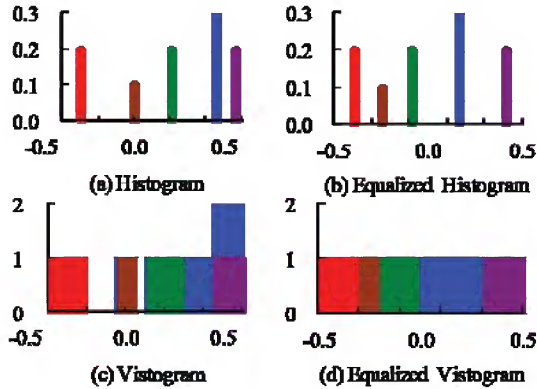


Figure 2: Histogram vs. vistogram equalization.

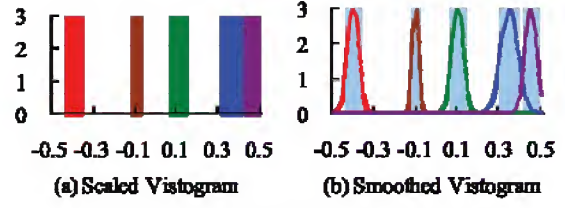


Figure 3: Scaled and smoothed vistograms.

anomalies a scaled smoothed version of vistogram is diffused (Figure 3).

To construct a scaled vistogram in three dimensions a scale parameter $s \in \mathbb{R}^+$, which is embedded into each hypercylinder of the vistogram, is chosen. This procedure adjusts the height and base volume of each four-dimensional hypercylinder, while its mass is preserved. Let $B(\mathbf{c}, R)$ be a d -dimensional ball of the radius R centered at \mathbf{c} . Then its volume integral, $V(R)$, is calculated as [12]

$$V(R) = \frac{4\pi}{3} R^3. \quad (0)$$

Let $u(\mathbf{x})$ be a uniform distribution function in $D = [b^-, b^+]^3$:

$$u(\mathbf{x}) := \begin{cases} 1 & : \mathbf{x} \in D \\ 0 & : \mathbf{x} \notin D, \end{cases} \quad (0)$$

and $B(\mathbf{x}; \mathbf{c}, r, s)$ be a scaled hypercylinder function of the radius r and the scale s centered at \mathbf{c} in D :

$$B(\mathbf{x}; \mathbf{c}, r, s) := \begin{cases} s^{-3} & : \|\mathbf{x} - \mathbf{c}\| \leq sr \\ 0 & : \|\mathbf{x} - \mathbf{c}\| > sr. \end{cases} \quad (0)$$

Then the mass of the scaled hypercylinder is $p = V(r)$. For a sufficiently small s all hypercylinders in the vistogram are reduced in size and do not overlap each other.

To approximate the scaled hypercylinder the Gaussian distribution function $g(\mathbf{x}; \boldsymbol{\mu}, \sigma^2 \mathbf{I})$ of \mathbf{x} with mean $\boldsymbol{\mu}$ and isotropic covariance $\sigma^2 \mathbf{I}$ (\mathbf{I} is a three-dimensional identity matrix) is employed

$$g(\mathbf{x}; \boldsymbol{\mu}, \sigma^2 \mathbf{I}) = \frac{1}{(\sqrt{2\pi}\sigma)^3} \exp\left\{-\frac{\|\mathbf{x} - \boldsymbol{\mu}\|^2}{2\sigma^2}\right\}. \quad (0)$$

To determine $\boldsymbol{\mu}$ and σ that fit $g(\mathbf{x}; \boldsymbol{\mu}, \sigma^2 \mathbf{I})$ to $B(\mathbf{x}; \mathbf{c}, r, s)$, their squared error is minimized. The hypercylinder of known volume p in three-dimensional vistogram is well approximated by the Gaussian function of the same weight, mean and standard deviation: $\sigma \propto \sqrt[3]{p}$. Hence, all hypercylinders can be converted into Gaussian functions.

For a given histogram $\{(\mathbf{x}_i, p_i)\}_{i=1}^n$ in the domain $D = [b^-, b^+]^3$, the probability density function is

$$f(\mathbf{x}; \mathbf{p}, s, \mathbf{X}) = \sum_{i=1}^n p_i g_i(\mathbf{x}), \quad (0)$$

where: $\mathbf{p} := (p_1, p_2, \dots, p_n)$ is the vector of n probabilities; \mathbf{X} is a concatenated vector of all \mathbf{x}_i 's;

$g_i(\mathbf{x}) := g_i(\mathbf{x}; \mathbf{x}_i, s^2 \sqrt[3]{p_i^2} \mathbf{I})$ is the i th component of MIG. The squared error of MIG from the uniform distribution is employed to measure the uniformity. The uniformity potential E for the uniform distribution is

$$E = \int_{\mathbb{R}^d} \left\{ u(\mathbf{x}) - \sum_{i=1}^n p_i g_i(\mathbf{x}) \right\}^2 d\mathbf{x} \quad (0)$$

$$= 1 - 2 \sum_{i=1}^n C_i + \sum_{i,j} S_{ij},$$

where: $C_i := \int_D p_i g_i(\mathbf{x}) d\mathbf{x}$ be the coherence of the i th component. It represents the volume of the i th component in D ; $S_{ij} := \int_{\mathbb{R}^d} p_i p_j g_i(\mathbf{x}) g_j(\mathbf{x}) d\mathbf{x}$ is the scattering of the i th and j th components. It represents their intersection volume. Let $C := \sum_{i=1}^n C_i$ and $S := \sum_{i,j} S_{ij}$ be total coherence and scattering potentials, respectively. Integrating the i th component of C_i

$$C_i := p_i \prod_{\xi=1}^3 G_{\xi,i}^{\Delta}, \quad (0)$$

where: $G_{\xi,i}^{\Delta} := G(b^+; \xi_i, s^2 \sqrt[3]{p_i^2}) - G(b^-; \xi_i, s^2 \sqrt[3]{p_i^2})$ is the definite integral of the marginal distribution of $g_i(\mathbf{x})$ with respect to ξ -coordinate ($\xi \in [b^-, b^+]$). Each term S_{ij} is

$$S_{ij} = \frac{p_i p_j}{(\sqrt{2\pi} s_{ij})^d} \exp \left\{ -\frac{\mathbf{z}_{ij}^T \mathbf{z}_{ij}}{2} \right\}, \quad (0)$$

where: $s_{ij}^2 := (\sqrt[3]{p_i^2} + \sqrt[3]{p_j^2}) s^2$ is the pooled-scale variance of the i th and j th Gaussian components, $\mathbf{z}_{ij} := (\mathbf{x}_i - \mathbf{x}_j) s_{ij}^{-1}$ is the pooled-scale displacement.

The histogram diffusion is a conservative system. Its uniformity potential E depends only on \mathbf{x}_i 's. Since the histogram is a set of particles of different masses, its total kinetic energy T is

$$T = \frac{1}{2} \sum_{i=1}^n p_i \dot{\mathbf{x}}_i^2. \quad (0)$$

The Euler-Lagrange formulation provides equation of motion for the histogram diffusion:

$$p_i \ddot{\mathbf{x}}_i = -\nabla_{\mathbf{x}_i} E = -\nabla_{\mathbf{x}_i} S + \nabla_{\mathbf{x}_i} C \text{ for } i=1, 2, \dots, n, \quad (0)$$

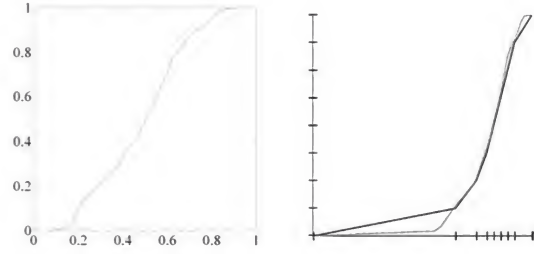
with a balancing constraint for the scaling factor s ,

$$\nabla_s S = \nabla_s C. \quad (0)$$

The histogram diffusion process is a nonlinear autonomous system of ODEs with a single time-independent constraint. The histogram diffusion process possesses valuable properties: i) dynamical and numerical stability, and ii) low computational complexity [13][14][15].

3. EXPERIMENTAL RESULTS

The histogram diffusion method provides almost the same mapping of the centralized GHE (0) as shown in Figure 5

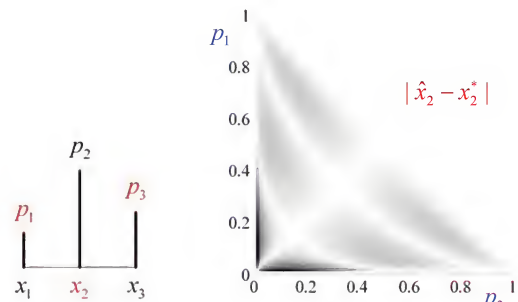


(a) Histogram diffusion (b) Mesh deformation [8]
Figure 5: GHEs for the Lena image.

(a). The equalized image resembles the image in Figure 1 (b). The histogram of the Lena image is positive at 219 gray values out of 256. Figure 5 (b) shows that the transformation function of GHE [8] is a piecewise linear approximation of cumulative histogram.

The error of 1D histogram diffusion from conventional GHE is calculated as the difference between the exact solution \mathbf{x}^* (0) and an actual solution $\hat{\mathbf{x}}$ that is obtained by minimization of (0). However, the solution $\hat{\mathbf{x}}$ cannot be obtained explicitly and, therefore, the true error cannot be calculated directly. Newton's method is used to estimate the standard error, but it does not provide a satisfactory estimate.

The canonical configuration of a 1D histogram is shown in Figure 4 (a) where $p_1 + p_2 + p_3 = 1$, $x_1 = 0.5(p_1 - 1)$ and $x_3 = 0.5(1 - p_3)$. It is assumed that p_2 does not interact with histogram values inside the domain. But it interacts with p_1 and p_3 at the end points. This assumption is valid only when the scaling factor is sufficiently small. The absolute error calculated as $|\hat{x}_2 - x_2^*|$ can be scaled down if $p_1 + p_2 + p_3 < 1$. Its projection on the plane $p_1 \times p_3$ is shown in Figure 4 (b). The intensity of shadowed areas corresponds to the value of absolute error, i.e., the black zone corresponds to the maximum value. The mean value of absolute error is 0.0126. It reaches a maximum of 0.5 for $0 < p_1 < 0.4$ or $0 < p_3 < 0.4$. The level of error is too small for the human eye to detect it in



(a) Canonical configuration (b) Absolute error $|\hat{x}_2 - x_2^*|$
Figure 4: Absolute error for a canonical configuration.

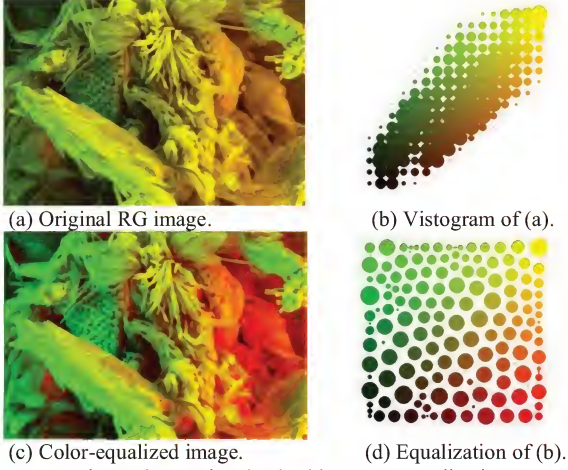


Figure 6: Two-band color histogram equalization.

equalized images.

Figure 6 (a) is the original (335×228) red-green image of the head of a moth [8]. It has two (R-red and G-green) 16 level bands. Its histogram is positive at 588 colors. The contrast of image is low because its histogram (Figure 6b) is dense along the diagonal. Using the histogram diffusion method the histogram was expanded to fit the uniform distribution. Figure 6 (c) and (d) show that the equalized image has higher contrast than the original image. The squared error of color-equalized image in Figure 6 (b) was 0.00615.

The results are compared to images reconstructed with the use of marginal CHE method. Figure 7 shows (768×512) images with 16 levels in each R, G, and B bands. Histograms of all images have 1501 colors. The image obtained with the marginal CHE method shows little enhancement of contrast compared to the original image. The image equalized with the proposed method shows even greater variety of colors compared to others. The squared error of color-equalized image in Figure 7 (b) was 0.092.

4. CONCLUSION

Histogram diffusion is developed and extends the GHE method to multi-dimension. As an alternative GHE the squared error of vistogram from the uniform distribution is minimized. To acquire smoothness, convexity and simplicity in mathematical formulation, all bars in the vistogram are approximated with Gaussian functions. As a result, the vistogram is approximated with a MIG. The histogram diffusion process is formulated as a nonlinear autonomous system of ODEs.

Results of histogram equalization for color images show the effectiveness of the histogram diffusion method. 1D histogram diffusion provides a solution which is nearly identical to conventional GHE and preserves the order of occurrences. Numerical error analysis of GHE and the

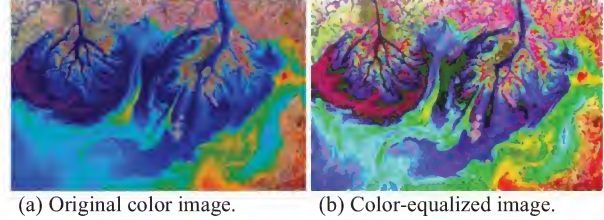


Figure 7: Histogram equalization of a color image.

histogram diffusion method with their canonical configurations shows the mean absolute error $\approx 1\%$. Results of histogram equalization of color images present uniform histograms and guarantee a greater variety of colors compared to original images.

5. REFERENCES

- [1] K. N. Plataniotis and A. N. Venetsanopoulos, *Color image processing and applications*, Springer Verlag, 2000.
- [2] R. E. Woods and R. C. Gonzalez, *Digital image processing*, Prentice Hall, 2nd ed. 2001.
- [3] A. A. Schwarz and J. M. Soha, Multidimensional histogram normalization contrast enhancement, *5th Canadian Symposium on Remote Sensing*, 1978:86-93.
- [4] I. M. Bockstein, Color equalization method and its application to color image processing, *Journal of Optical Society of America*, 3(5):735-737, 1986.
- [5] W. F. McDonnell, R. N. Strickland, and C. S. Kim, Digital color image enhancement base on the saturation component, *Optical Engineering*, 26(7):609-616, 1987.
- [6] J. Duan and G. Qiu, Novel histogram processing for colour image enhancement, *International Conference on Image and Graphics*, 2004.
- [7] P. A. Mlsna and J. J. Rodriguez, Explosion of multidimensional image histograms, *International Conference on Image Processing*, 3:958-962, 1994.
- [8] E. Pichon, M. Niethammer, and G. Sapiro, Color histogram equalization through mesh deformation. *International Conference on Image Processing*, 2:117-120, 2003.
- [9] A. K. Forrest, Color histogram equalization of multi-channel images, *IEE Proceedings - Vision, Image, and Signal Processing*, 152(6): 677-686, 2005.
- [10] T. Kim and H. S. Yang, Color histogram equalization via least-squares fitting of isotropic Gaussian mixture to uniform distribution, *Electronics Letters*, 42(8):452-453, 2006.
- [11] T. Kim and H. S. Yang, Multidimensional histogram equalization by fitting isotropic Gaussian mixture to uniform distribution, *Intl. Conference on Image Processing*, 2006.
- [12] S. Sykora, Volume Integrals over n -Dimensional Ellipsoids, In *Stan's Library*, Ed. S. Sykora, 1, 2005.
- [13] C. L. Dym, *Stability Theory and Its Applications to Structural Mechanics*, Dover Publications, 2002.
- [14] W. Walter, *Differential and Integral Inequalities*, Springer-Verlag, New York, 1970.
- [15] D. Halperin and M. H. Overmars, Spheres and Molecules and Hidden Surface Removal, *10th Ann. ACM Symp. Computational Geometry*, 113-122, 1994.
- [16] T. Kim, Histogram Equalization by Gaussian Particle Diffusion, *Electronics Letters*, 2010, 46(13): 911-913.